Combined in situ and remote sensing of ionospheric ion outflow

S. A. Fuselier,[1] E. S. Claflin,[1] S. B. Mende,[2] C. W. Carlson,[2] and T. E. Moore[3]

Received 12 July 2005; revised 9 December 2005; accepted 3 January 2006; published 18 February 2006.

[1] Images of charge-exchanged neutrals from ion outflow during a period of substorm recovery are supported by auroral oval images and simultaneous in situ ion outflow measurements. From these combined remote sensing and in situ measurements, the ion outflow is shown to consist of ion conics. The energy of these conics likely increases from <10 eV at 0.7 R_E to >10 eV above this altitude. These first global images of the instantaneous outflow show that outflow occurs over nearly the entire dayside auroral oval at high latitudes, including the cusp. The broad local time extent of the outflow is observed for ~2.5 hours. Outflow on the nightside may be weaker than on the dayside and/or may have different energy-altitude dependence. **Citation:** Fuselier, S. A., E. S. Claflin, S. B. Mende, C. W. Carlson, and T. E. Moore (2006), Combined in situ and remote sensing of ionospheric ion outflow, *Geophys. Res. Lett.*, *33*, L04103, doi:10.1029/2005GL024055.

1. Introduction

[2] Polar orbiting spacecraft have observed ionospheric ion outflow (e.g., H^+, He^+, and O^+) along high latitude field lines for decades (see, e.g., *Yau et al.* [1985] and the review by *Hultqvist et al.* [1999]). These snapshots in space and time have been used to study many statistical properties of the outflow. For example, studies show that the outflow flux is proportional to magnetospheric activity and solar cycle [*Yau et al.*, 1985]. More recent statistical studies indicate that outflow fluxes scale directly with the Poynting flux into the ionosphere and with the "soft" electron density (i.e., precipitating electrons with E <~1 keV) [*Strangeway et al.*, 2005].

[3] Two types of ion outflow distributions with distinct pitch angle characteristics and energies of 10s of eV are typically observed. The first type, ion beams, has peak flux along the magnetic field and the second type, ion conics, has peak flux at an angle to the magnetic field. For conics in the northern hemisphere, this conic angle is typically ~130° [e.g., *Peterson et al.*, 1992]. Ion conics have been the focus of intense study because their properties provide clues to the acceleration mechanisms that extract them from the ionosphere.

[4] Statistical studies show that conics occur in the auroral zone between invariant latitude 65–85°, at all local times, but preferentially on the morning/dayside between 5 and ~13 magnetic local time (MLT), and at altitudes from ~1 to >4R_E [*Kondo et al.*, 1990; *Miyake et al.*, 1996]. Over this altitude range, conic angles are nearly constant [*Peterson et al.*, 1992]. Since the magnetic field strength decreases dramatically from 1 to 4 R_E altitude, there must be continuous perpendicular energization to maintain the constant pitch angle with altitude. In general, this perpendicular energization leads to higher average temperatures at higher altitudes; however, low energy conics (<1 keV) still occur over these altitudes with nearly equal probability [*Hultqvist et al.*, 1999, and references therein]. Finally, the properties of H^+ and O^+ conics are similar [e.g., *Kondo et al.*, 1990].

[5] In situ measurements have revealed important statistical properties of ion outflow. However, the nature of in situ snapshots at a single MLT and altitude, taken over a few minutes, precludes determining the temporal and spatial variation of ion outflow over important timescales (such as the substorm timescale of ~1 hour). Statistical studies show that ionospheric ion outflow [*Yau et al.*, 1985] and ionospheric ions in the plasma sheet [e.g., *Lennartsson*, 1992] both depend on magnetospheric activity. Thus, there is a strong indication that the ionosphere influences the plasma content of the plasma sheet (and ring current) during a substorm.

[6] With no spatial and temporal information over substorm timescales, two disparate models for the outflow that populates the plasma sheet have been developed. The first model has the plasma sheet supplied by outflow from the entire auroral oval, with approximately equal contributions from the dayside and nightside [*Shelley*, 1985]. The second model has the plasma sheet supplied largely by outflow from the dayside cusp region [*Moore et al.*, 1985]. Neither model predicts when and how long the outflow will occur, only that it increases early in the substorm process.

[7] As outflow propagates along the magnetic field line, some ions charge exchange with the geocorona. If the resulting neutral atoms have energies from 10 eV to ~300 eV, then they can be imaged with the low energy neutral atom (LENA) imager on the IMAGE spacecraft [*Moore et al.*, 2000]. Ideally, the images can be inverted to determine the global properties of the parent ion populations. In practice, this inversion has proven difficult because of the characteristics of the parent outflow distributions [*Fuselier et al.*, 2002]. In particular, it is difficult to determine if neutral flux changes are due to changes in intensity, temperature (energy), charge exchange altitude, and/or pitch angle of the parent ion population. Of these, pitch angle and energy appear to be very important [*Fuselier et al.*, 2002].

[8] This paper reports a combination of neutral atom imaging, in situ measurements of ion outflow, and auroral imaging that eliminates much (but not all) of

[1]Lockheed Martin Advanced Technology Center, Palo Alto, California, USA.
[2]Space Science Laboratory, University of California, Berkeley, California, USA.
[3]Goddard Space Flight Center, Greenbelt, Maryland, USA.

0094-8276/06/2005GL024055$05.00

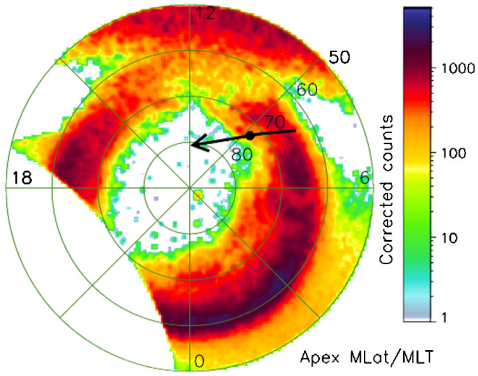

Figure 1. Auroral oval during a substorm recovery interval on 27 November 2000. The black arrow shows the FAST spacecraft trajectory. At the dot on this trajectory, intense ion outflow was observed.

the uncertainty associated with using only one of these techniques.

2. Ion Outflow Observations

[9] Figure 1 shows the auroral intensity from the IMAGE/FUV Wideband Imaging Camera (WIC) [*Mende et al.*, 2000] on 27 Nov 2000 at 0212 UT. At the time of the image, the spacecraft was located on the dawnside at ~4 R_E altitude. The auroral oval is shown in MLT – invariant latitude coordinates with noon at the top and dusk to the left. There is no oval from ~18 to 23 MLT because, at this low altitude, the WIC field-of-view does not cover the entire oval. The WIC detects emissions from 140–180 nm, produced mainly by precipitating electrons. In addition, there are dayglow emissions from 09–15 MLT up to the terminator (at ~60° invariant latitude). The auroral oval is extensive, stretching from 60° to ~80° invariant latitude over almost all MLT except noon. This extended oval is typically observed during the substorm recovery phase [e.g., *Mende et al.*, 2003].

[10] During these auroral observations, the Fast Auroral SnapshoT (FAST) spacecraft traversed the dawnside oval at ~4000 km altitude (see the arrow in Figure 1). Figure 2 shows FAST in situ observations of ion and electron precipitation and ion outflow. The four panels show (top to bottom) the precipitating ion flux (in an energy-time format), the precipitating electron flux, the ionospheric ion outflow (within 30° of anti-parallel), and the outflow pitch angle versus time (for E > 50 eV). From 0204 to 0213 UT, the FAST spacecraft traversed the auroral oval from low to high latitude, observing >100 eV ion precipitation. The poleward edge of the oval has intense fluxes of soft (E < 1 keV) electron precipitation and ionospheric ion outflow at energies primarily <10 eV but extending to ~100 eV. The dot on the FAST spacecraft trajectory in Figure 1 shows the location of this intense outflow. (The apparent intense fluxes in Figure 2 at 0220 UT are a spacecraft charging effect and are not polar cap outflow.) The pitch angle plot in Figure 2 shows that, for E > 50 eV, the intense ion outflow at 0212 UT peaks between ~100° and ~150° from the magnetic field (i.e., the ion outflow distributions are conics). Ion conics at the poleward edge of the oval are observed during substorm recovery [e.g., *Mende et al.*, 2003] and are associated with soft electron precipitation [*Strangeway et al.*, 2005].

[11] Figure 3 shows a neutral atom image from the LENA imager taken from 0210 to 0220 UT. The time delay from low altitude to the IMAGE spacecraft for 50 eV Hydrogen is ~6 min. Thus, this image is centered on the intense ion outflow observed by the FAST spacecraft. Plotted are counts/s of neutral atoms from ~10 eV to <300 eV viewed from the IMAGE spacecraft location on the dawnside. Magnetospheric magnetic field lines at L-shells of 2 and 4 are shown in the sunward, duskward, tailward, and dawnward directions (counterclockwise from the lower right hand corner). Neutral flux is seen at all MLTs, but the most intense fluxes encircle half the Earth from 06 to 18 MLT. This type of neutral flux is seen often when the IMAGE spacecraft is post-perigee during a substorm recovery interval and this image is representative of images taken from 0100 UT (just after perigee) to 0330 UT.

[12] Some neutral flux in Figure 3 is associated with charge exchange of the ionospheric ion outflow observed by the FAST spacecraft at 09 MLT. Outflow from the high latitude edge of the auroral oval (Figure 2) at E > 10 eV that charge exchanges at high altitudes (~2–3 R_E) would appear in the lower part of Figure 3 between the sunward and dawnward field lines. Figure 4 shows that the apparent arrival direction of charge-exchanged ions that had a pitch angle of 129° at the time of neutralization would appear to be offset from the Earth direction in the LENA image. Thus, there is a direct association between the intense outflow seen at low altitudes by the FAST spacecraft and the charge

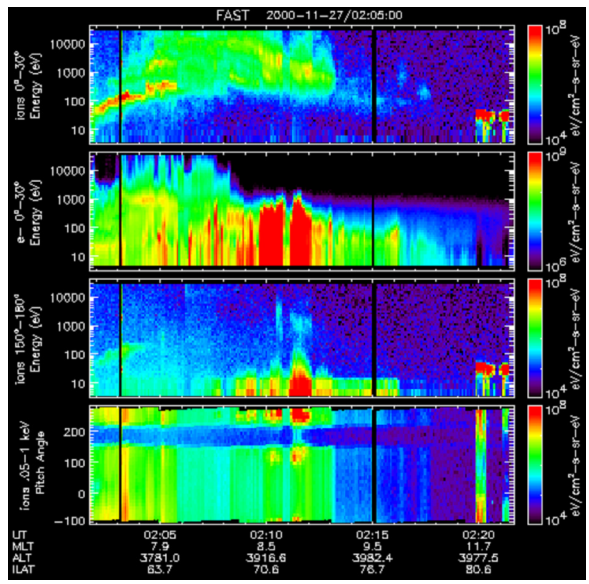

Figure 2. FAST spacecraft in situ observations. (top to bottom) Ion precipitation, electron precipitation, ionospheric ion outflow, and pitch angles of the outflow. In the auroral oval (from 0202 and 0213 UT) there is intense ion and electron precipitation. At the poleward edge of the oval, intense low energy electron precipitation is associated with peak ion outflow (ion conics) at E < 10 eV.

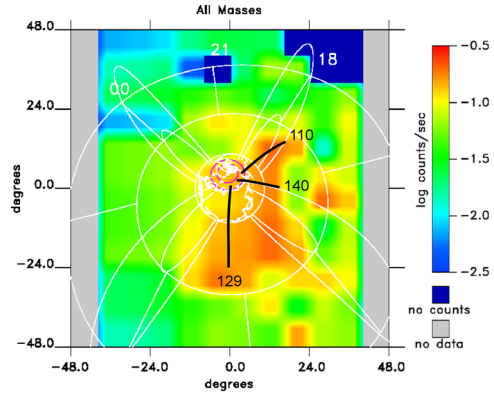

Figure 3. Neutral atom image from the IMAGE spacecraft. Noon (dawn) is in the lower right (left) hand corner. The neutral flux peaks over the entire dayside off the direction to the Earth. Three magnetic field lines from 72° latitude and from 0900, 1200, and 1500 MLT are identified by the pitch angle (129°, 140°, and 110°, respectively) for charge exchange at three different altitudes.

exchanged neutrals from high altitudes in the lower middle part of the LENA image.

3. Understanding the Dayside Ionospheric Outflow

[13] The LENA image in Figure 3 also shows charge-exchanged ionospheric outflow from other parts of the auroral oval. The three black lines in the figure are model magnetic field lines that originate from 72° latitude and from 09, 12, and 15 MLT (counterclockwise from the field line labeled 129°). These black field lines terminate at 2.8, 1.9, and 1.3 R_E and the pitch angles at the termination (129°, 140°, and 110°, respectively) are labeled in Figure 3. The 72° invariant latitude corresponds to the latitude where FAST observed intense ion outflow (at 09 MLT in Figure 2). These field line tracings, the FAST observations, and previous statistical studies suggest the following interpretation of the LENA image in Figure 3: Ion outflow occurs from ~0730 to ~1500 MLT. This outflow occurs at high latitudes (>70°) and consists of ion conics with conic angles from ~100° to 150°. The ion conic angle remains fixed with altitude from ~0.7 R_E (the FAST spacecraft location) up to several R_E. Below the FAST altitude, the ion conics have energies <10 eV, but above this altitude, the conic energy increases significantly. As the ion conic altitude increases, they charge exchange with the hydrogen geocorona. The resulting neutrals retain the pitch angle and energy of the parent ion population. High neutral fluxes are observed where the LENA imager energy range (10–~300 eV) and field of view intersects the energy and pitch angle ranges of the parent ion population.

[14] Figure 5 quantifies this charge exchange altitude – pitch angle relationship. The curves of constant pitch angle from 100°–150° were obtained by tracing the magnetic field lines (e.g., in Figure 3) at 72° latitude and computing the pitch angle versus altitude along the field line. The range of observable pitch angles is different for each MLT because the IMAGE spacecraft is on the dawnside.

[15] In general, pitch angles decrease with increasing charge exchange altitude. It is easiest to interpret Figure 5 at 09 MLT, where the FAST spacecraft observed ion outflow at 72° latitude and with a range of pitch angles from 100°–150°. Figure 3 shows that although the FAST spacecraft observes pitch angles down to ~100°, the minimum pitch angle for the neutral flux is ~130°. The difference between the parent ion population and the observed neutral flux has at least two interpretations. One is that the ion conics fold with altitude along the magnetic field, so that at ~3R_E, the flux at 100°–120° is significantly reduced. A second interpretation is that, the decreasing geocoronal density with altitude results in less charge exchange until the resulting neutral flux is below the sensitivity limit of the LENA imager. Since folding of ion conics is not observed statistically [*Peterson et al.*, 1992], the second interpretation is favored.

[16] The neutral flux profile at other MLT also favors the second interpretation. Assuming intense ion outflow at 72° latitude at the other MLT, a nearly constant maximum altitude of ~3 R_E for the neutral flux is obtained, independent of pitch angle. The differences in the dawnside and duskside pitch angles are a result of viewing geometry. Only a narrow range of pitch angles is seen on the dawnside, but nearly the full range of pitch angles, is observed for the outflow from ~1300 MLT. By 1500 MLT, the maximum observable altitude of the neutral flux is determined by the minimum conic angle of ~100°.

[17] Figure 3 shows that there is also a minimum altitude for the observed neutral flux. Independent of the parent ion population characteristics, the neutral flux should be highest closest to the Earth, where the geocoronal density is highest. The neutral flux peaks off the Earth direction (i.e., at higher altitudes) because of the energy and pitch angle characteristics of the parent ion population. At 09 MLT, the neutral flux peaks off the Earth direction because the parent ion conic population would require high fluxes at pitch angles >150° (Figure 5). At ~14 MLT, neutrals with pitch angles <150° would be observed at low altitudes (Figure 5). The fact that they are not suggests that the ion conic energy is <~10 eV (i.e., below the LENA imager minimum energy) for altitudes <~1 R_E.

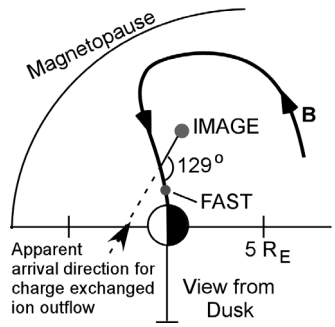

Figure 4. Duskside view of the magnetic field line associated with intense ion outflow (ion conics at 129°). Charge exchange at altitudes above the FAST spacecraft results in an apparent arrival direction at IMAGE that is off the Earth direction.

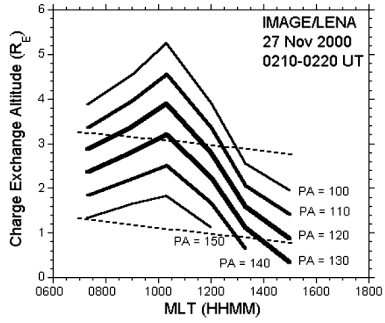

Figure 5. Charge exchange altitude versus MLT for outflow at 72° latitude. Higher altitudes (and further from the Earth in Figure 3), have smaller pitch angles. LENA observes neutrals from 0730 to 1500 MLT and from altitudes between the dashed lines.

[18] The above interpretation of the LENA image in Figure 3 assumes outflow at a fixed 72° latitude. If outflow occurs at lower latitudes at MLT other than 09 (i.e., where the FAST spacecraft observed outflow), then the pitch angle curves in Figure 5 shift to lower charge exchange altitudes. For example, outflow at 67° instead of 72° would shift the 100° pitch angle curve between the 110° and 120° curve positions. The neutral atom image in Figure 3 is inconsistent with a large shift (i.e., >5°) in the outflow latitude. For such a shift, the neutral flux from 15 MLT would be seen at ion conic angles <90° (i.e., no longer moving anti-parallel to the magnetic field line).

4. Discussion

[19] Using FAST spacecraft in situ observations (Figure 2) of ion outflow from the poleward edge of the auroral oval as a guide, the arrival direction of the neutrals (Figure 3) is consistent with high altitude charge exchange of ion outflow that originated from the poleward edge of the auroral oval (Figure 1) from ~0730 to 1500 MLT.

[20] The neutral arrival direction (Figure 3) and the range of conic pitch angles observed by the FAST spacecraft (Figure 2) indicate that the LENA imager is not seeing charge-exchange outflow below ~1 R_E altitude on the duskside. Charge exchange is certainly taking place at lower altitudes, where the geocorona is denser. However, if the parent ion population has energies <10 eV, then the resulting neutrals will be below the ~10 eV low energy threshold of the LENA imager. Indeed, the intense outflow seen by the FAST spacecraft at ~0.7 R_E has peak energies <10 eV. These observations suggest that ion conics are energized from energies <10 eV at ~0.7 R_E to >10 eV at ~1 R_E.

[21] The LENA image (Figure 3) also shows no emissions above ~3 R_E altitude. This maximum altitude is likely associated with the decrease in the geocorona density with altitude and, ultimately, the sensitivity of the LENA imager.

[22] Figure 3 is the first global image of conic ion outflow during a substorm recovery interval. It shows that the outflow occurs over a broad range of dayside local times that encompasses, but is not limited to the cusp. Furthermore, Figure 3 is representative of many images taken over ~2.5 hours, indicating that the broad local time extent remains stable over a long time period. The local time range (Figure 3) and the ~72° latitude of the outflow (Figure 2) are consistent with the peak in the soft electron precipitation on the dayside from a statistical study [*Chaston et al.*, 2003].

[23] The Chaston et al. study shows significant soft electron precipitation on the nightside as well. In contrast, the LENA image (Figure 3) shows significantly less neutral atom flux on the nightside than on the dayside. There are a number of possible reasons why the nightside neutral flux is lower. They range from reduced ion outflow to pitch angle and/or energy-altitude differences in the nightside parent ion population. Unfortunately, without supplemental information on the parent ion population on the nightside, the neutral atom image in Figure 3 cannot be used to determine the dominant reason. Another limitation of these LENA images is that they focus on ion conics. Although intense conic outflow is seen in situ at 09 MLT (Figure 2), non-conic ion outflow may occur at other local times. One place where this is possible is the cusp, where field-aligned beam ion outflow would be all but invisible to LENA unless the imager looked directly along the magnetic field.

[24] In summary, the observations show that, at least for substorm recovery, conic ion outflow is not confined to the cusp region. Further work is needed to correlate neutral atom images and ion outflow during other phases of the substorm cycle.

[25] **Acknowledgments.** The IMAGE mission is the result of the work of a large number of dedicated scientists and engineers. Research at LMATC was supported by contracts from GSFC and UC, Berkeley.

References

Chaston, C. C., J. W. Bonnell, C. W. Carlson, J. P. McFadden, R. E. Ergun, and R. J. Strangeway (2003), Properties of small-scale Alfvén waves and accelerated electrons from FAST, *J. Geophys. Res.*, *108*(A4), 8003, doi:10.1029/2002JA009420.

Fuselier, S. A., H. L. Collin, A. G. Ghielmetti, E. S. Claflin, T. E. Moore, M. R. Collier, H. Frey, and S. B. Mende (2002), Localized ion outflow in response to a solar wind pressure pulse, *J. Geophys. Res.*, *107*(A8), 1203, doi:10.1029/2001JA000297.

Hultqvist, B., M. Øieroset, G. Paschmann, and R. Treumann (Eds.) (1999), *Magnetospheric Plasma Sources and Losses, Space Sci. Ser.*, vol. 6, 496 pp., Springer, New York.

Kondo, T., B. A. Whalen, A. W. Yau, and W. K. Peterson (1990), Statistical analysis of upflowing ion beam and conic distributions at DE 1 altitudes, *J. Geophys. Res.*, *95*, 12,091–12,102.

Lennartsson, O. W. (1992), A scenario for solar wind penetration of Earth's magnetic tail based on ion composition data from the ISEE 1 spacecraft, *J. Geophys. Res.*, *97*, 19,222–19,238.

Mende, S. B., et al. (2000), Far ultraviolet imaging from the IMAGE spacecraft. 2. Wideband FUV imaging, in *The IMAGE Mission*, edited by J. L. Burch, pp. 271–285, Springer, New York.

Mende, S. B., C. W. Carlson, H. U. Frey, T. J. Immel, and J.-C. Gérard (2003), IMAGE FUV and in situ FAST particle observations of substorm aurorae, *J. Geophys. Res.*, *108*(A4), 8010, doi:10.1029/2002JA009413.

Miyake, W., T. Mukai, and N. Kaya (1996), On the origins of the upward shift of elevated (bimodal) ion conics in velocity space, *J. Geophys. Res.*, *101*(A12), 26,961–26,970.

Moore, T. E., C. R. Chappell, M. Lockwood, and J. H. Waite Jr. (1985), Superthermal ion signatures of auroral acceleration processes, *J. Geophys. Res.*, *90*, 1611–1618.

Moore, T. E., et al. (2000), The low-energy neutral atom imager for IMAGE, in *The IMAGE Mission*, edited by J. L. Burch, pp. 155–195, Springer, New York.

Peterson, W. K., H. L. Collin, M. F. Doherty, and C. M. Bjorklund (1992), O^+ and He^+ restricted and extended (bi-modal) ion conic distributions, *Geophys. Res. Lett.*, *19*, 1439–1442.

Shelley, E. G. (1985), Circulation of energetic ions of terrestrial origin in the magnetosphere, *Adv. Space Res.*, *5*, 401.

Strangeway, R. J., R. E. Ergun, Y.-J. Su, C. W. Carlson, and R. C. Elphic (2005), Factors controlling ionospheric outflows as observed at intermediate altitudes, *J. Geophys. Res.*, *110*, A03221, doi:10.1029/2004JA010829.

Yau, A. W., P. H. Beckwith, W. K. Peterson, and E. G. Shelley (1985), Long-term (solar cycle) and seasonal variations of upflowing ionospheric ion events at DE 1 altitudes, *J. Geophys. Res.*, *90*, 6395–6407.

C. W. Carlson and S. B. Mende, Space Science Laboratory, University of California, Berkeley, Berkeley, CA 94720-7450, USA.

E. S. Claflin and S. A. Fuselier, Lockheed Martin Advanced Technology Center, Palo Alto, CA 94304-1191, USA. (fusilier@spasci.com)

T. E. Moore, Goddard Space Flight Center, Greenbelt, MD 20771, USA.